 doi: 10.1111/j.1365-246X.2007.03459.x

Estimation of an optimum velocity model in the Calabro-Peloritan mountains—assessment of the variance of model parameters and variability of earthquake locations

H. Langer,[1] R. Raffaele,[2] A. Scaltrito[1] and L. Scarfi[1]

[1] *Istituto Nazionale di Geofisica e Vulcanologia – Sez. di Catania, Piazza Roma* 2, I-95123 *Catania, Italy. E-mail: scarfi@ct.ingv.it*
[2] *Dipartimento di Scienze Geologiche, University of Catania, Corso Italia* 57, I-95129 *Catania, Italy*

Accepted 2007 March 28. Received 2007 March 28; in original form 2006 April 28

SUMMARY

Accurate earthquake locations are of primary importance when studying the seismicity of a given area, they allow important inferences on the ongoing seismo-tectonics. Both, for standard, as well as for earthquake relative location techniques, the velocity parameters are kept fixed to *a priori* values, that are assumed to be correct, and the observed traveltime residuals are minimized by adjusting the hypocentral parameters. However, the use of an unsuitable velocity model, can introduce systematic errors in the hypocentre location. Precise hypocentre locations and error estimate, therefore, require the simultaneous solution of both velocity and hypocentral parameters.

We perform a simultaneous inversion of both the velocity structure and the hypocentre location in NE-Sicily and SW-Calabria (Italy). Since the density of the network is not sufficient for the identification of the 3-D structure with a resolution of interest here, we restrict ourselves to a 1-D inversion using the well-known code VELEST. A main goal of the paper is the analysis of the stability of the inverted model parameters. For this purpose we carry out a series of tests concerning the initial guesses of the velocity structure and locations used in the inversion. We further assess the uncertainties which originate from the finiteness of the available data set carrying out resampling experiments. From these tests we conclude that the data catalogue is sufficient to constrain the inversion. We note that the uncertainties of the inverted velocities increases with depth. On the other hand the inverted velocity structure depends decisively on the initial guess as they tend to maintain the overall shape of the starting model. In order to obtain an improved starting model we derive a guess for the probable depth of the Moho. For this purpose, we exploit considerations of the depth distribution of earthquake foci and of the shear strength of rock depending on its rheological behaviour at depth. In a second step we derive a smooth starting model and repeated the inversion. Strong discontinuities tend to attract hypocentre locations which may introduce biases to the earthquake location. Using the smooth starting model we obtaine again a rather smooth model as final solution which gives the best traveltime residuals among all models discussed in this paper. This poses severe questions as to the significance of velocity discontinuities inferred from rather vague *a priori* information. Besides this, the use of those smooth models widely avoids the problems of hypocentre locations being affected by sudden velocity jumps, an effect which can be extremely disturbing in relative location procedures. The differences of the velocity structure obtained with different starting models is larger than those encountered during the bootstrap test. This underscores the importance of the choice of the initial guess. Fortunately the effects of the uncertainties discussed here on the final locations turned out as limited, that is, less than 1 km for the horizontal coordinates and less than 2 km for the depth.

Key words: earthquake location, inverse problem, seismic velocities, seismology, statistical methods.

INTRODUCTION

The area of northeastern Sicily and southern Calabria is one of the Italian regions with the highest hazard (see, e.g. Monaco & Tortorici 2000). Historically it experienced several destructive earthquakes (e.g. 1908 December 28) with estimated magnitudes of about 7 or higher (see, e.g. Monaco & Tortorici 2000). The seismicity in the area has been discussed in various hypothesis and interpretation has been on the seismotectonic patterns in the region (Neri *et al.* 2003, 2005; Billi *et al.* 2006; Sgroi *et al.* 2006).

The significance of seismicity patterns can be considerably improved with relative location procedures, such as HypoDD as proposed by Waldhauser & Ellsworth (2000) or master event methods (see, e.g. Frémont & Malone 1987). Using relative locations techniques Scarfi *et al*. (2005) recently demonstrated that in this area some of the trends visible in the hypocentre distribution might be partly an effect of a location bias rather than representing a genuine tectonic feature. In fact, scattered clouds of hypocentres may literally collapse to small volumes with an extent of no more than some hundreds of metres. Moreover, the large number of high quality microearthquake records, available from local seismic networks, discloses the possibility to exploit them for the inversion of seismic velocity models and to compare them to findings from other geological and geophysical disciplines. An important issue in this context is the identification of a suitable velocity model. Neglecting the coupling between hypocentral and velocity parameters during the location process, can indeed introduce systematic errors in the hypocentre location (Thurber 1992; Eberhart-Phillips & Michael 1993), which strongly depend on the assumed *a priori* velocity structure (Kissling *et al.* 1995). The problem of biases introduced by the uncertainties of the velocity parameters is relevant both for absolute and relative location techniques as was recently underscored by Michelini & Lomax (2004), who discuss the effect of the choice of an unsuitable velocity model in relative location. The simultaneous solution of both the earthquake location problem as well as the inversion of the velocity structure is a way to tackle drawbacks with location techniques using models where the velocity parameters are kept fixed to *a priori* values.

For NE-Sicily and SW-Calabria *a priori* information concerning the velocity structure is available from coarse scale tomographic investigations which cover wide parts of the southern Tyrrhenian sea and adjacent areas (De Luca *et al.* 1997; Neri *et al.* 2002; Barberi *et al.* 2004). Other information reported in literature comes from analyses of limited portions of few DSS profiles (Deep seismic sounding experiment, see Cernobori *et al.* 1996; Nicolich *et al.* 2000).

Our study concerns the seismicity and the velocity modelling of the region stretching from the Gulf of Patti towards the Messina Strait and Aspromonte Mountain, which is a much smaller area than the one considered in the afore mentioned papers of De Luca *et al*. (1997), Neri *et al*. (2002) or Barberi *et al*. (2004). Most of the stations available for earthquake location, however, lie outside the epicentre area of the events and the density of the network does not allow a 3-D tomography with a resolution of interest here. We therefore, limit ourselves to a 1-D inversion of the velocity structure using the VELEST code developed by Kissling (1995).

Besides the identification of a 1-D model for NE-Sicily and SW-Calabria—which is of importance for a reliable location—we focus on the stability of the inverted model parameters. For this purpose we carry out a series of tests concerning the initial guesses of the velocity structure and locations used in the inversion. In particular, we try to exclude events whose location is unstable in the sense that it has various solutions with equivalent goodness of fit. On the other hand we are aware that the seismic catalogue used here is itself a subset of the earthquakes occurred in the area, and forms—at best—a random sample of an underlying parent population of seismic events. In other words, the results of our inversion may vary when we consider data recorded in different time span even if the assumption holds that our data set forms a representative sample of the parent population of all seismic events. A way to assess the uncertainties which originate from the finiteness of the available data sets, is the use of resampling experiments among which the so-called 'bootstrap' method is the most general one (see, e.g. Efron 1982). The bootstrap method consists in creating new data sets drawing randomly samples from an existing sample set. During the resampling each item of the original set has equal probability at any time to pass to the new data set ('sampling with replacement'). Thus, it may happen that certain samples occur several times in the new data set, whereas others do not appear at all. As a consequence, some information now is redundant. This is not considered as a drawback as earthquakes indeed tend to occur in clusters, thus redundancy of information is an intrinsic feature of our inversion problem. As a result of the bootstrap resampling we get a number of velocity models for which we obtain statistical parameters as averages, medians and confidence intervals. We can exploit examples not occurring in bootstrapped catalogues for purposes of cross-validation tests as these were not used during the inversion. The goal is to find out whether the results are reproducible. Cross-validation is of particular importance in models with a high number of degrees of freedom where the problem of 'overfitting' exists (i.e. the model is said to 'fit noise').

SEISMOTECTONIC SETTING

The investigated region belongs to the Calabro-Peloritan Arc which is a part of the Apennine-Maghrebian orogenic belt, along the Africa–Europe Plate boundary. The Arc connects the NW–SE-trending southern Apennines with the WSW-striking Maghrebian thrust zones (Fig. 1). Its recent geodynamic evolution has been closely related to the opening of the Tyrrhenian sea beginning in the middle Miocene, the ESE-ward drift of the Calabro-Peloritan massif and the subduction of Ionian lithosphere. This southeast-directed migration process was accommodated by roughly NW–SE-striking fault systems in the southernmost Tyrrhenian area and northeastern Sicily (Finetti & Del Ben 1986).

The seismicity of the arc is characterized by the occurrence of both crustal (depth $\lesssim$30 km) and subcrustal (depth $\gtrsim$30 km) earthquakes. The latter are located beneath the southern Tyrrhenian sea, to the east of the fault system stretching from the Aeolian Islands across the site of Tindari to the city of Giardini on the Ionian coast (ATG system hereafter). In the last three centuries, this area was the theatre of large damaging earthquakes, such as the 1783, 1905 and 1908 earthquakes, with maximum MCS intensities of X–XI and estimated magnitudes ranging from 6 to 7.4 (Fig. 1, see e.g. Monaco & Tortorici 2000). The fault plane solutions available for the Messina-Reggio Calabria earthquake (1908 December 28; M = 7.1, Gasparini *et al.* 1985) as well as those obtained for smaller events in southern Calabria (1978 March 11; M = 5.6, Dziewonski *et al.* 1987) and in the Gulf of Patti (1978 April 15; M = 5.6, Gasparini *et al.* 1985) are consistent with an ESE–WNW extension. Recently, Neri *et al*. (2003) identified two tectonic subareas of seismic deformation: the area to the west of the ATG is dominated by a compressional regime presumably induced by plate convergence.

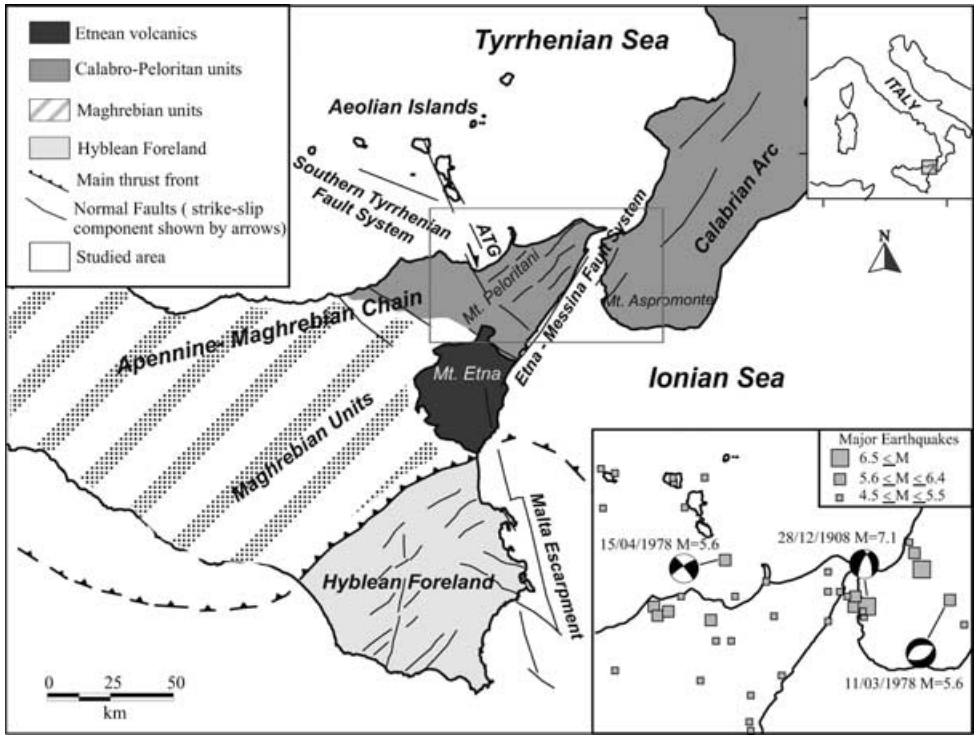

Figure 1. Simplified tectonic and structural map of Sicily and southern Calabria (from Lentini *et al.* 2000; Monaco & Tortorici 2000). The small map to the lower right shows the location of major earthquakes in the area of interest and some focal solutions, (Gasparini *et al.* 1985; Dziewonski *et al.* 1987).

Conversely, the area to the east of the ATG is characterized by NW–SE extension which can be related to an Ionian subduction slab rollback.

DATA SET

The Calabro-Peloritan permanent network, managed by Istituto Nazionale di Geofisica e Vulcanologia (INGV), consists of eight three-component seismic stations (see Fig. 2). These stations are equipped with short-period seismometers, having a natural frequency of 1 Hz and a damping of 70 per cent of critical. The data are transmitted to the data acquisition centre via radio telemetry. The sampling frequency of the signal and the anti-alias filter corner frequency are, respectively, 125 and 35 Hz. During 2003, some of the stations were replaced by new digital ones, equipped with broadband (40 s) three-component sensors, with a dynamic range of 144 dB. In order to reduce the azimuthal gap, we have been using stations deployed on the Aeolian Islands and on the northern flanks of Mt Etna. Where possible, we added data from the national permanent seismic network. All the stations use the same base time, set by GPS time.

Between 1994 and 2005, about 600 earthquakes were located in northeastern Sicily and southern Calabria (see web site of INGV—http://www.ct.ingv.it/GridTerremoti.htm). Their duration magnitudes which were estimated using a relation by Caltabiano *et al*. (1986), range from 1.0 to 3.8. The map and the cross-sections of the earthquakes are displayed in Fig. 2. For our purpose, we selected only well located events matching minimum requests with respect to location quality, that is, events with at least five well readable *P*-, two clear *S*-arrivals and with a maximum azimuthal gap of 180°. On average 14 pickings were available for each event. We further rejected all events with root mean square (rms) residuals larger than 0.25 s and standard location errors (Erh and Erz) larger than 2.5 km. Moreover, if two or more events were belonging to a multiplet family with similar waveform, we maintained only a representative member choosing the one with the highest number of observations. This both improves the overall quality of the data set and, at the same time, limits undesired effects of redundancy, which may artificially overrate zones with earthquake clusters with respect those where the distribution of hypocentres is dispersed over wider area.

A major problem is the identification of a good start solution for the hypocentre locations and the assessment of the sensitivity of the inversion process in this respect. For this aim, before including the earthquakes in the joint inversion of velocity and hypocentral parameters, we tested the location stability—using the VELEST code but keeping the velocity parameters fixed—by shifting the trial hypocentres randomly in the space, up to ±6 km for the hypocentre spatial coordinates. This helped us to identify events for which different locations with equivalent traveltime residuals can be found. Note that the presence of events with unstable locations bears the risk of introducing biases as the inversion process may decrease the traveltime residuals by shifting around the hypocentre coordinates instead of adjusting the velocity model parameters properly.

In practice, we have been comparing the original locations and the relocations which were obtained using initial hypocentres whose coordinates were subjected to a random perturbation (Husen *et al.* 1999). We repeated the test five times and considered the realizations where the difference between the solutions were maximum. In doing so, we get a conservative estimate of the stability of the hypocentre locations by removing events with horizontal or vertical location variations greater than 3 km. All tests revealed fairly stable epicentre determinations for the majority of the events. In fact, the differences of the results between original start locations and the randomly perturbed ones was fairly low (1 km or less for 80 per cent

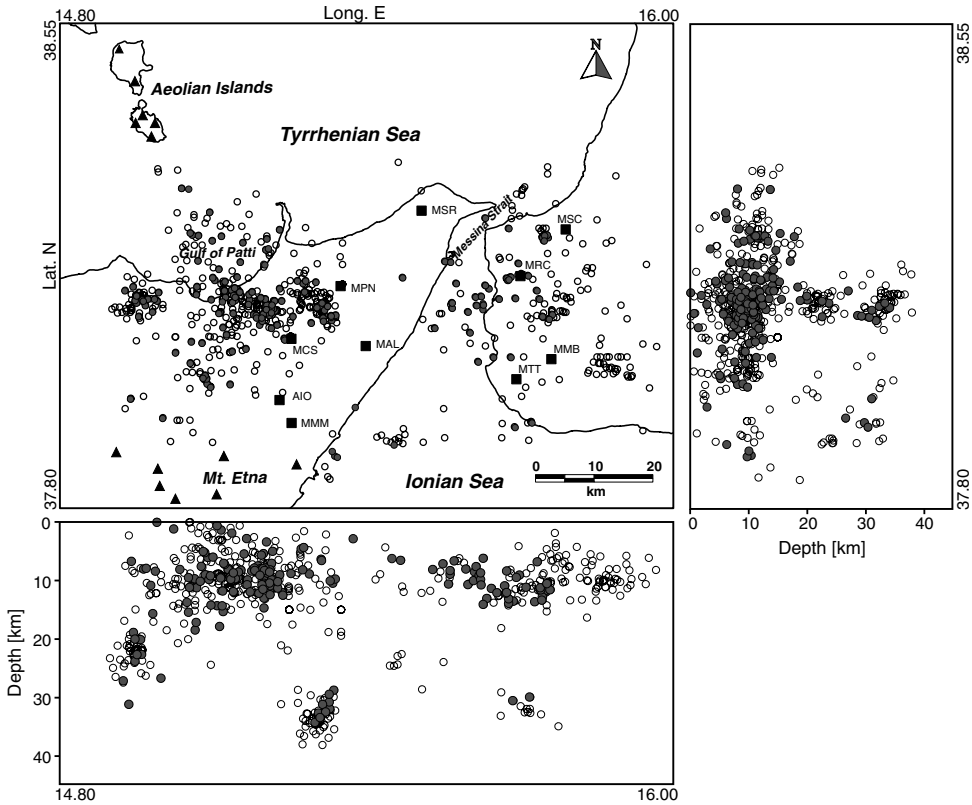

Figure 2. Map view, N–S and E–W cross-sections of the earthquakes (circles) located in the studied area in the time span from 1994 to 2005. Dark circles indicate the data set selected for this study. Permanent seismic networks: (i) NE Sicily and southern Calabria and (ii) Mt Etna and Aeolian Islands, are indicated by squares and triangles, respectively.

of the events, see Fig. 3). After the above selection process, our data set consisted of 181 well locatable events, with a total of 1757 *P*- and 780 *S*-observations (Fig. 2).

CALCULATION OF A MINIMUM 1-D MODEL

For the identification of an optimum 1-D *P*-velocity model we have been using the widely known software VELEST (Kissling 1995). In this approach, both hypocentre locations as well as the parameters of the velocity structure and station corrections are inverted, using the global misfit (sum over all traveltime residuals) as a measure for the goodness of fit.

A common problem here, as in many other inversion problems, is the dependence of the results from the initial guess. Having eliminated events which can be suspected to depend strongly on the initial solution, we focus on the identification of the starting model for the inversion of the velocity structure. Following the suggestion of Kissling *et al*. (1994), we collected all available *a priori* information regarding the impedance structure of the area under study (velocities and layer thickness). A major feature of the Calabro-Peloritan region is the high-gradient crustal thinning from inner lands of Sicily and Calabria (35–40 km) to the Tyrrhenian basins (10 km) (Dezes & Ziegler 2001). Other information available in literature comes from analyses of limited portions of few DSS profiles (Cernobori *et al.* 1996; Nicolich *et al.* 2000) and tomographic investigations (De Luca *et al.* 1997; Neri *et al.* 2002; Barberi *et al.* 2004). Because the geology of Calabro-Peloritan area is very complex and the region confines with different tectonic provinces (i.e. Etna and Aeolian Islands), we considered several 1-D *a priori* models (see Fig. 4):

The models from 1 to 6 are directly derived from the studies of De Luca *et al*. (1997), whereas in the models 7 and 8 we surmise the presence of velocity gradients, similarly to the model used in Scarfì *et al*. (2005). *S*-phases were included in the inversion procedure by simply assuming a constant *Vp*/*Vs* ratio (1.75). We refrained from inverting *S*-wave velocities and used a fixed *Vp*/*Vs* value because the number of *S*-wave onsets was limited. Thus, *S*-wave readings were used only to better constrain the earthquake location, in particular the focal depth (see, e.g. Laigle 1998).

Considerable differences are encountered in the solutions obtained for the various starting models (see Figs 4 and 5). In all cases we note a significant increase of the goodness of fit (decrease of traveltime residuals, see Table 1). At the end we obtain the highest degree of fit using the initial models 4, 5 or 8, with residuals of *ca.* 100 ms. For the sake of simplicity we shall focus our further discussion on model 4. The general tendencies with respect to station corrections and statistical considerations, however, remain essentially valid also for the other two models, that is, 5 and 8.

STATION CORRECTIONS

Station corrections are an integral part of the optimum 1-D inversion. Typically they are referred to a 'reference station', which is chosen preferably close to the geometrical centre of the network, and is among the stations with the highest number of readings. The reference station is assigned to a correction value of 0. Negative corrections are encountered when the true velocities are supposed to be

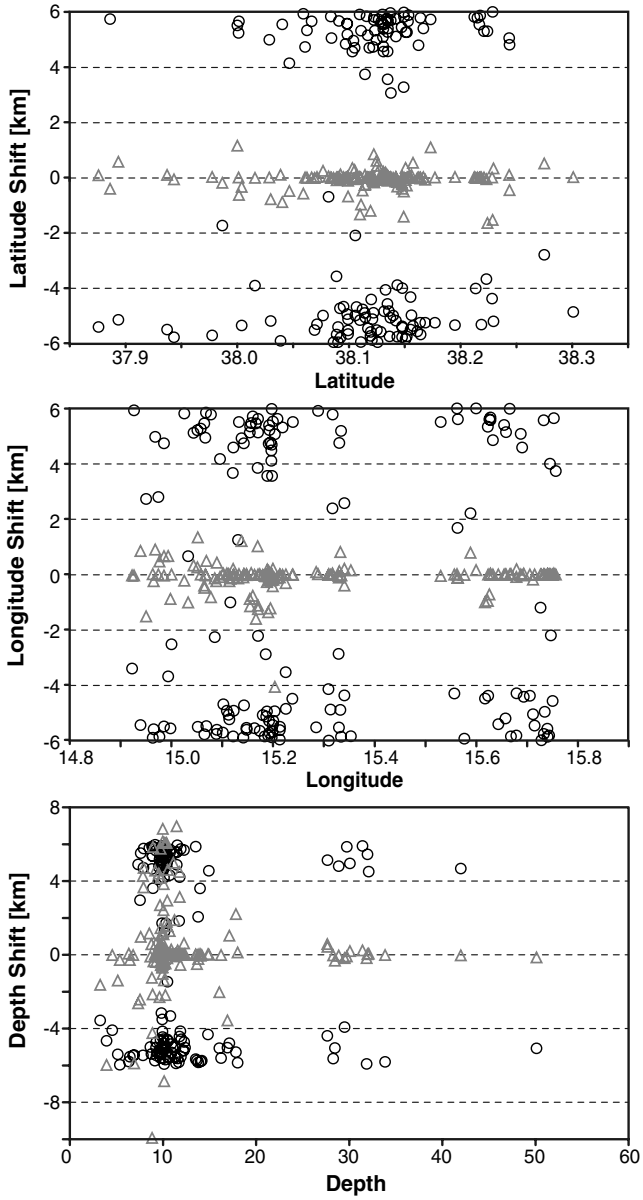

Figure 3. Hypocentre stability test. Black circles: maximum coordinate differences between perturbed and start original locations encountered during the five random experiments. Grey triangles: maximum differences of final locations (see text for more details).

higher, positive correction occur for lower velocities than predicted by the model. We may exclude biases on the station corrections due to topographic effects since VELEST allows to use station elevations for the joint inversion of hypocentral and velocity parameters. Consequently rays are traced exactly to the true station position (Husen *et al.* 1999).

The distribution of negative or positive station corrections reflects to some part the overall three-dimensionality of the velocity field (Kissling *et al.* 1995). In fact, our network is composed of stations deployed in different tectonic units. Mt Etna, in the southern part of the seismic network, is a complex stratovolcano, over 3300 m high, based on a sedimentary cover which itself has a thickness of several thousands of metres. The Peloritani Mountains consist mainly of highly metamorphic rocks, with local sedimentary basins where weaker material may reach thicknesses of several hundreds of metres (see, e.g. Lentini *et al.* 2000). In the southern Tyrrhenian sea with the Eolian Islands we note, besides peculiar geological surface conditions, a decrease of the thickness of the crust, with a Moho depth of 22 km in the area of the island of Lipari, and reaching as few as 10 km in the central part of the Tyrrhenian Basin (Dezes & Ziegler 2001)

In Fig. 6, we report the station corrections encountered for the model 4. We identify two major tendencies. All stations on Mt Etna have positive correction values, indicating a delayed arrival of *P*-waves as expected for the optimum 1-D model, whereas they scatter around −0.1 s in the Calabro-Peloritan Mountains and in the Eolian Islands. In the Calabro-Peloritan Mountains we note slight, but nevertheless systematic differences between stations which are placed on highly metamorphic rock and those in the afore mentioned local sedimentary basins. However, the scatter of the corrections obtained with the various starting models did not exceed 0.1 s.

BOOTSTRAP ASSESSMENT OF THE VARIANCE OF THE VELOCITY STRUCTURE, STATION CORRECTIONS AND EARTHQUAKE LOCATIONS

The high computational capacities nowadays available disclose the possibility to examine the stability of even complex schemes of calculus carrying out numerical experiments under various assumptions of disturbance and lack of knowledge concerning the controlling parameters. In the paragraphs above we have been discussing the role of the initial solutions (both with respect to the velocity structure as well as the hypocentre locations). A further source of uncertainty, however, is the finiteness of the data set. As in any statistical problem, the significance of inverted models increases with the amount of available data. In other words, the standard deviation of inverted model parameters should be inversely dependent on the size of the data set. Unfortunately, in inversion problems there is no simple rule—such as the central limit theorem valid for the estimation of averages—which could be used for the estimation of the standard deviations of our calculated model parameters. A way out is given by resampling techniques; in particular the bootstrap method. This method consists in creating new data sets drawing randomly samples from an existing sample set. Resampling is carried out following a scheme known as 'sampling with replacement', that is, a chosen element of the data set is not withdrawn and can be selected repeatedly. Among others, we point out the following advantages of resampling methods over more conventional ones (see, e.g. Hesterberg *et al.* 2003).

(1) *Fewer assumptions:* for instance, resampling methods do not require *a priori* assumptions on the distribution of the underlying parent population.

(2) *Generality:* resampling methods are similar for a wide range of statistics, and do not require analytic expressions for each statistic.

(3) Immediate understanding of the concepts of resampling methods as they are formally simple.

(4) Resampling methods have proven to give results being coherent with statistics for which the analytical solutions are known.

For our purposes, we bootstrapped our earthquake data set 80 times and carried out the optimum 1-D inversion with each newly generated data set, starting from the *a priori* model 4. From the distribution of velocities shown in Fig. 7(a) and (b), we learned that our original model is pretty close to the median of the ones obtained with the bootstrapped data catalogues. In the first 20 km the standard

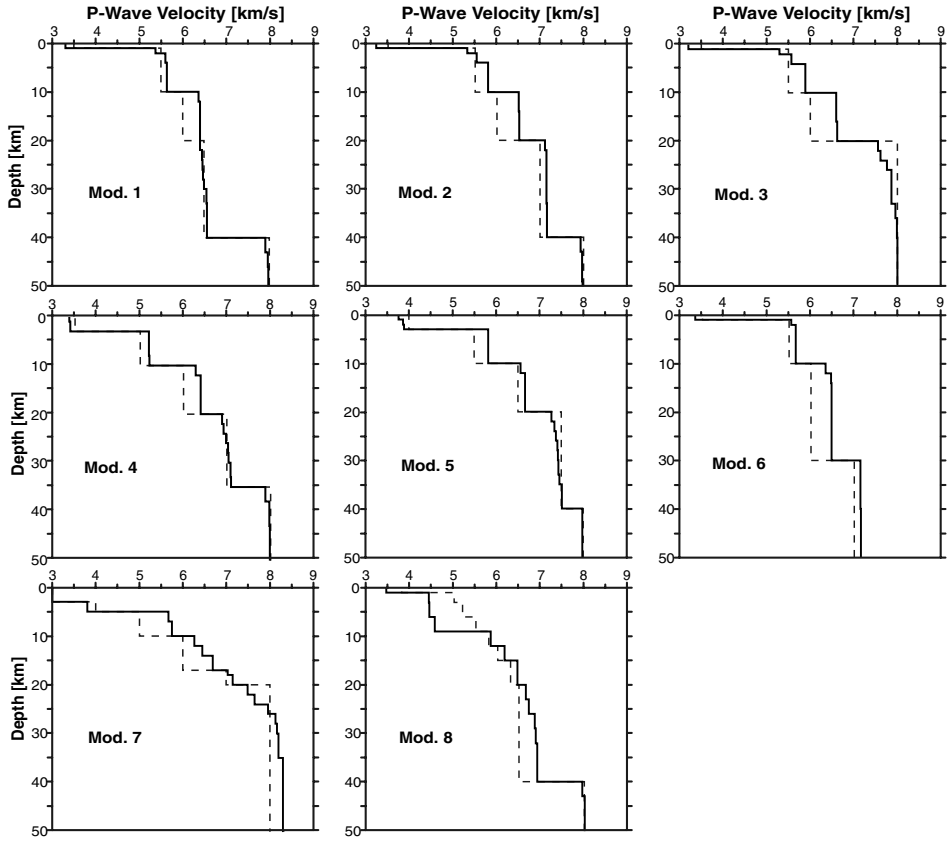

Figure 4. Initial 1-D velocity models (dashed lines) and computed minimum 1-D velocity models (solid lines).

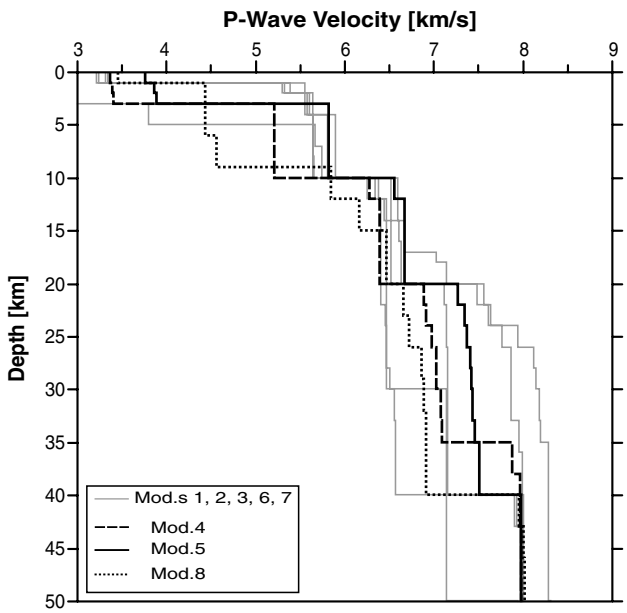

Figure 5. Comparison between the computed minimum 1-D velocity models. Emphasis is given to the models 4, 5 and 8 which showed the best performance.

deviation of the velocities is found between 60 and *ca.* 100 m s^{-1}, at greater depth this scatter increases to over 200 m s^{-1} (see Fig. 7d). Besides this, we note considerable differences in the shape of the statistical distribution of the velocities in the parts above and below 20 km. Whereas in the shallower parts of the structure the distribution of velocities can be roughly considered to be Gaussian, that is, showing low values of both skewness and curtosis, the values for these higher statistical moments are considerably higher below 20 km (Fig. 7c).

Similarly to the previous paragraph, we consider the statistics of the station corrections obtained for the 80 inversions carried out with the bootstrapped data catalogues. Again we note positive station correction values for stations on Mt Etna, slightly negative ones for the stations on the Calabro-Peloritan Mountains and on the Eolian Islands. Both absolute values and scatter are found of the same order as during the inversions with the various starting models.

We may finally examine how the variations of the velocity structure affect the final hypocentre locations. Certain events are affected more than others, quiet independently on the models found during the bootstrap experiment. Considering the maximum scatter obtained for each event, we get the statistics reported in Table 2.

CROSS-VALIDATION

We can understand any inversion as some kind of supervized learning problem, where we try to adjust model parameters in the sense that a specific set of observations is fitted minimizing the prediction error, obtained from the difference between calculated and observed data. The number of model parameters, however, is typically fixed *a priori*, exploiting our existing ideas about the structure of the model we are looking for. In our case the model parameters concern the velocity structure. Besides this, we have to account for the hypocentre coordinates and origin times of the earthquakes which further increase the number of degrees of freedom of our inversion problem.

Table 1. Start and final traveltime residuals for each used model.

	MOD1	MOD2	MOD3	MOD4	MOD5	MOD6	MOD7	MOD8
Start	0.195	0.194	0.200	0.242	0.188	0.195	0.367	0.354
Final	0.105	0.104	0.105	0.100	0.101	0.113	0.135	0.100

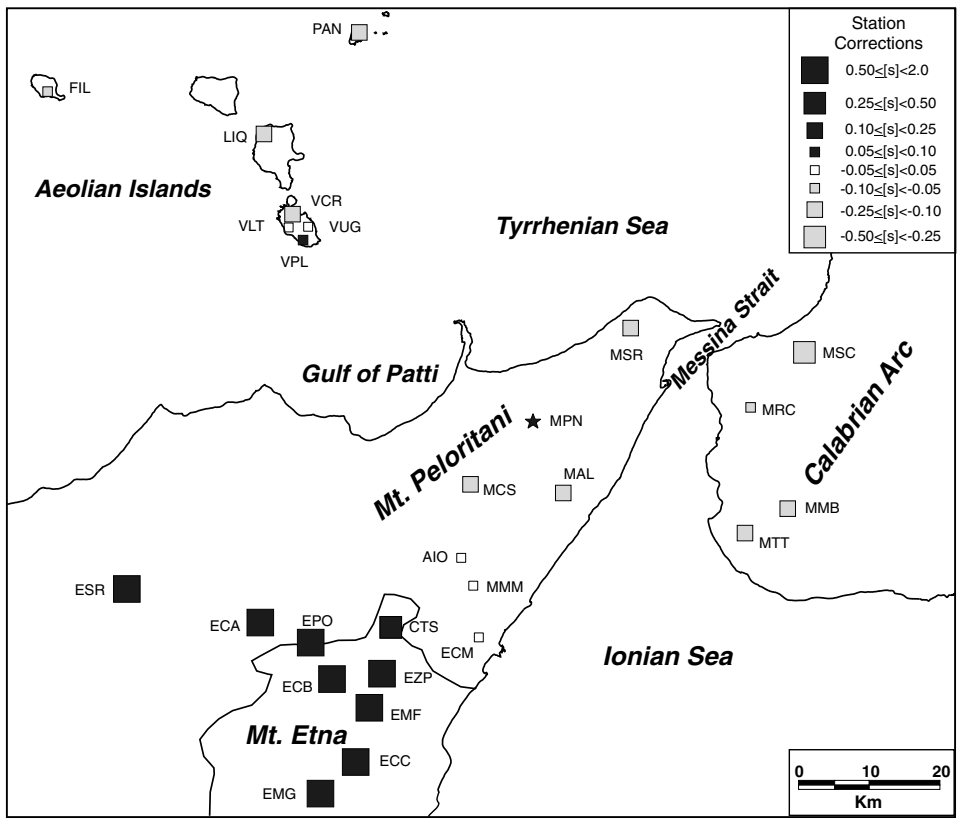

Figure 6. Station corrections computed with the minimum 1-D velocity model 4. The star indicates the 'reference station'. Negative corrections correspond to the true velocities faster than the model.

It is well known that the prediction error tends to decrease as the number of degrees of freedom increase. However, we are left with the question whether all these model parameters are necessary and give a significant improvement of the prediction error. Even worse, complex model may exhibit a very unpleasant effect, called 'over-fitting'. In this case the prediction error decreases to low values for the data set which is used for the estimation of the model parameters. When applied to other data not used so far, these models give unstable results, even though these new data may belong to the same parent population as the data used during the inversion.

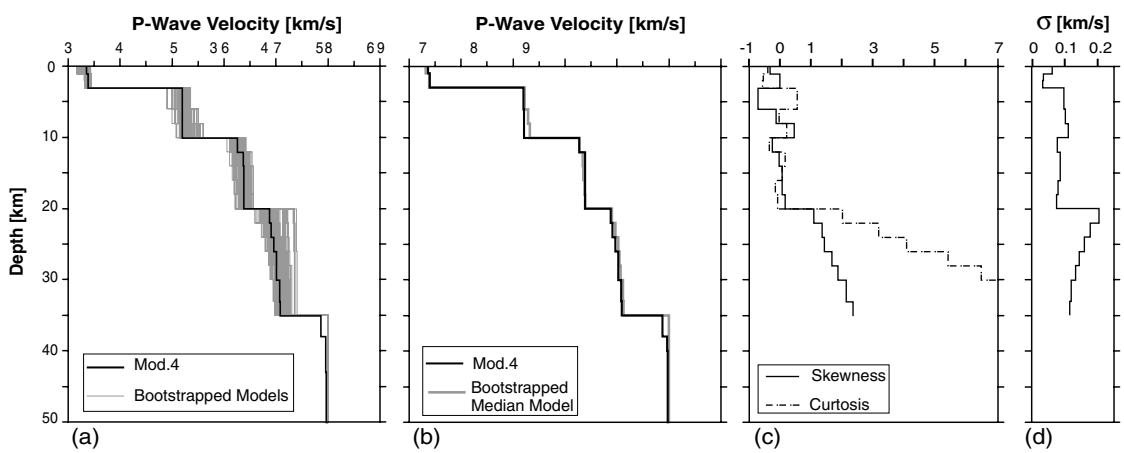

Figure 7. (a and b) Comparison between the minimum 1-D velocity model 4 and those derived from the data sets generated using the bootstrap resampling technique (see text for more details). (c and d) Statistical parameters of the velocities for the bootstrapped models.

Table 2. Variation of the hypocentre locations during the bootstrap experiment.

	$\leq$1 km	$\leq$2 km	>2 km
Percentage of Events (Long.)	82.3	13.3	4.4
Percentage of Events (Lat.)	91.2	6.1	2.8
Percentage of Events (Depth)	50.3	27.6	22.1

There are various concepts reported in the literature which cope with the problem of the trade-off between model complexity and the goodness of fit, such as the 'Akaike Information Criterion', and the 'Bayesian Information Criterion'. We address the reader to textbooks of statistical learning (see, e.g. Hastie *et al.* 2002). Here we have been following the cross-validation method, which is a straight forward strategy to assess a generalized prediction error as it is based on the use of an extra sample data set, often referred to as 'test set'. We prefer it to other concepts because it fits well into the general strategy of the present paper, where we try to assess the model performance using as little *a priori* information about the statistical characteristics of our problem as possible. In cross-validation, part of the available data are used to fit a model, whereas another part—let's say, one-fifth—is set aside for the estimation of the prediction error. The procedure is repeated according to the relation between number of test and total number of available date. For instance, choosing one-fifth of the data for test, cross-validation is repeated at least five times, selecting in each run different examples for the test data set. With a comparatively large test set one obtains a stable estimation of the prediction error, in other words, its estimate has a low variance. As the part of the data available for fitting the model is lower with a large test data, the prediction error tends to be higher than the error expected when all data are used for the model fit. In other words it has a bias towards an overestimation. In the 'leave-one-out' strategy only one sample is used for testing, whereas the remaining (i.e. almost all) data are used for fitting the model. Cross-validation in this strategy has to be repeated N times, where N is the number of available data. In the leave-one-out-strategy the estimated prediction error is approximately unbiased but can have a high variance, as the training data sets are so similar (see Hastie *et al.* 2002).

Recall that the resampling of the original data catalogue was carried out as 'sampling with replacement', consequently a part of events appears several times in the resampled set, others not at all. We may, therefore, exploit the bootstrap experiments for a cross-validation of the model performance. For large data sets the number of not sampled elements during bootstrapping converges to Ne^{-1} (N being the total number of elements in a set), that is 36.8 per cent of the total number of events (*cf.* Hastie *et al.* 2002). In order to assess the stability of our inversion, we have been using the results with the original data set as a reference, and compared the deviation of the hypocentre locations obtained both for events sampled during bootstrapping (referred to as 'training events') and the non-sampled ones ('test events'). During the bootstrap process every event has a probability of theoretically in 63.2 per cent for being in the training set, and 36.8 per cent for making part of the test set. This implies that our error estimates are on the safe side as they may be overestimated to some degree. As we bootstrapped 80 times, each event appears during a number of runs in the set of training events, in other runs in the set of test events. We thus may monitor the deviations for each event depending on to which set it belongs (see Fig. 8).

Averaging over all bootstrap runs, we find the goodness of fit for both training and test events, measured from the traveltime residuals, only slightly differs from the ones obtained using the total data set. On average the goodness of fit obtained for each single events deviates around 15 ms from the one obtained with the original data set, regardless whether the event belonged to the set of training or test events. When considering for each event the worst residuals encountered during 80 bootstrap runs, the average deviation is 35 ms. In terms of average location differences, we have 330 and 370 m for latitude and longitude, and 520 m for the depth for the test set. Averaging as before over the largest encountered deviations the corresponding values are, 650 and 1150 m. Similar deviations are found for the training set. Averaging over all 80 bootstrap runs we obtain 330 and 360 m for latitude and longitude, and 520 m for depth. For the largest deviation we find 580, 710 and 1290 m, respectively. In Fig. 8, we note that, except for single events, the trends for test and training set are very similar.

FINAL OPTIMUM MODEL

From the bootstrap and cross-validation experiments we conclude that the data set is large enough to provide a fairly stable inversion. All models obtained during the bootstrap test cluster around a median model, which is close to the one obtained with start model 4, maintaining basic characteristics of the start model. The observation that the inverted models strongly reflect the characteristics of the initial guess was observed also in the majority of the other models considered in this paper (see Fig. 4). This rises questions as to the significance of the position of the discontinuities assumed *a priori*, in particular the ones at depths of 4, 10 and 20 km, as well as the Mohorovicic discontinuity ('Moho'), which remain in their original positions also in the inverted models.

An independent evidence for the position of the Moho can be obtained from the frequency distribution of the foci as a function of depth. As we recognize in Fig. 2, the gross of our foci is concentrated in a depth range less than 20 km. Beyond this depth only few locations are found. A further maximum of earthquake foci is present in a range between 30 and 40 km. The occurrence of such a side maximum of earthquake foci is possible under certain rheological and thermodynamic conditions.

First we remember that for the generation of earthquakes it is necessary that the shear strength of rock is controlled by its brittle behaviour. The depth dependence of brittle strength is commonly described by 'Byerlee's law' (see Fig. 9)

$$\tau_c = 0.85\ \sigma_n$$

with τ_c being the shear strength, σ_n = the normal stress acting on a plane; at larger depth, where τ_c is over 200 MPa

$$\tau_c = 60\ \text{MPa} + 0.6\ \sigma_n.$$

On the other hand, with increasing temperature ductile behaviour becomes relevant and the strength of the lithosphere is controlled by a power law (or 'Dorn's law'):

$$d\varepsilon/\text{dt} = \sigma_d^n\, A\, \exp(-Q/RT),$$

where $d\epsilon/dt$ is the strain rate, σ_d the differential stress, n, A, Q are material parameters (see Table 3), R the Boltzmann gas constant, and T the temperature in K. The power law is an empirical relation for ductile deformation and has to be modified in some cases. For olivine above differential stress $\sigma_1 - \sigma_3 > 200$ MPa, Goetze (1978) suggested the following relation (referred to as 'modified Dorn's law')

$$\sigma_1 - \sigma_3 = \sigma_D \left(1 - \left[RT/Q_D^* \{\ln(d_{\varepsilon D}/dt) - \ln(d_\varepsilon/dt)\}\right]^{1/2}\right)$$

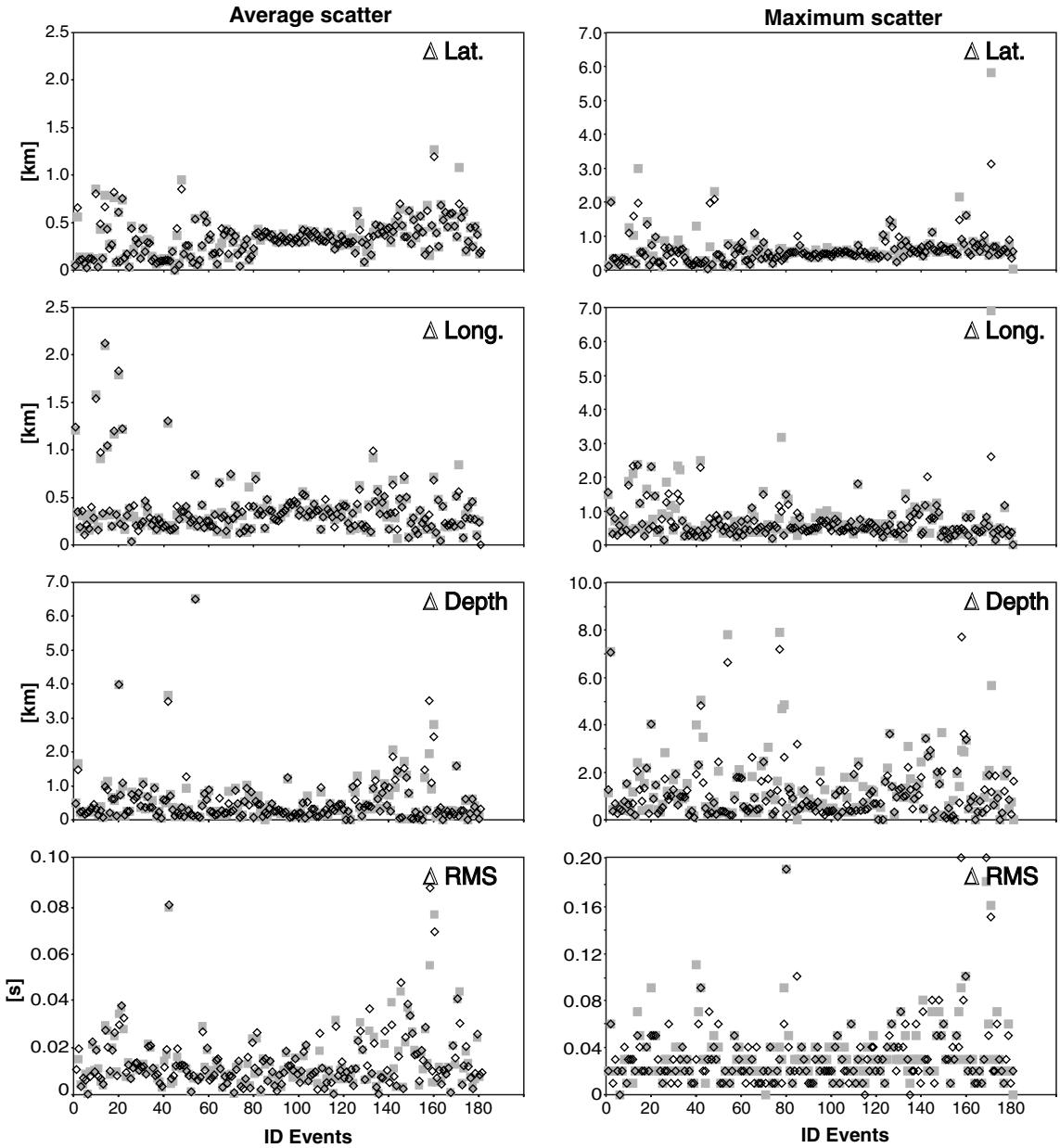

Figure 8. Scatter of hypocentre locations using the bootstrapped models. On the left, the average values, on the right the maximum values for each event. Grey squares and black rhombuses indicate 'training' and 'test' events, respectively.

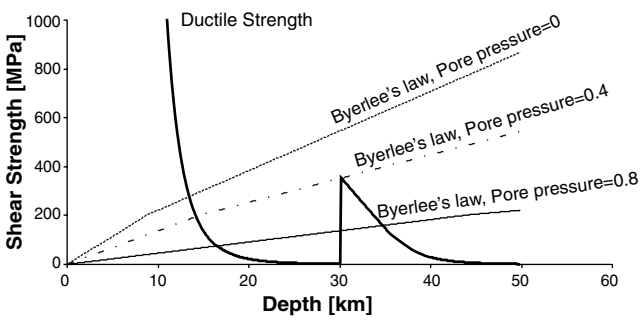

Figure 9. Shear strength of a 'Brace-Goetze Lithosphere'. The fat line represents shear strength calculated assuming a ductile behaviour of rock. The straight lines are given by 'Byerlee's law' of brittle shear strength assuming pore pressure parameters of 0, 0.4 and 0.8, respectively.

which is by far less temperature dependent than the original Dorn's law. The equations given above allow us to set up simple rheological models of the lithosphere as a whole.

An interesting model for our present case is the so called 'Brace-Goetze Lithosphere', which is sketched in Fig. 9 using the parameters shown in Table 3. In the crust we have been assuming that ductile strength is essentially controlled by quartz. For depth below the Moho we used the parameters for olivine (see for instance, Stüwe 2002 for more details). We assumed a standard deformation rate for our area of 3×10^{-15} s^{-1} . This value was derived from deformation measurements reported by D'Agostino and Selvaggi (2004) and corresponds to an accumulating dislocation of 2 m across 20 km (parameters roughly corresponding to a $M = 7$ earthquake; see Wells & Coppersmith 1994) in 1000 yr. Following the sketch of the shear strength with depth, we first note a brittle regime where

Table 3. Controlling parameters for the 'Brace-Goetze Lithosphere'.

Parameter	Value/unit	Description
	Dorn's or power law	
A (Quartz)	5×10^{-6} MPa^{-3}s^{-1}	Pre-exponent constant
Q (Quartz)	1.9×10^{5} J mol^{-1}	Activation energy
n	3	Power exponent
A (Olivine)	7×10^{4} Mpa^{-3}s^{-1}	Pre-exponent constant
Q (Olivine)	5.2×10^{5} J mol^{-1}	Activation energy
	Modified Dorn's law	
Q (Olivine)	5.4×10^{5} J mol^{-1}	Activation energy
$d\epsilon_D/dt$	5.7×10^{11}	Critical strain rate
σ_D	8500 MPa	Critical stress
dt/dZ	20 °K km^{-1}	Temperature gradient (see ftp://ftp.ngdc.noaa.gov/Solid˙Earth/Global_Heatflow/)
$d\epsilon/dt$	3×10^{-15} s^{-1}	Deformation rate, gives *ca.* 2 m/20 km in 1000 yr

the shear strength increases with depth. The depth where brittle and ductile strength have the same magnitude is called the brittle/ductile transition. In theory, this depth delimits the possibility for the occurrence of earthquakes. Using a pore pressure of 0.8 we obtain a first brittle/ductile transition, that is, a delimiting level for the possibility of earthquakes, at a depth of *ca.* 17 km. At the Moho we have a transition of rock composition from sialic to mafic, where olivine plays a dominant role. Due to the change in material properties, ductile shear strength is again greater than predicted brittle shear strength, especially when we assume a pore pressure of 0.4 or 0.8. Hence, material failure is again controlled by brittle behaviour and earthquakes are again possible. Assuming a Moho depth of 30 km, that is, in a depth where we again note the occurrence of earthquakes, we infer that brittle fracture is possible, for pore pressure 0.8, in a depth range between 30 and about 36 km. There's plenty of uncertainty with respect to the controlling parameters of the rheological behaviour of the lithosphere, such as the material parameters, the deformation rate, the geothermal gradient at greater depth, etc. Nonetheless our simple calculations show, that the occurrence of earthquakes right underneath the Moho can be explained under reasonable assumptions. In particular, the occurrence of foci at those levels is facilitated in environments with extensional tectonics, which is valid for the area under study. Further, the cluster of the earthquakes in question occurred as a swarm (see Scarfì *et al.* 2005) which entails the role of fluids supporting a high pore pressure, such as 0.8 postulated Fig. 9.

For the other major *a priori* discontinuities at 4, 10 and 20 km we have no clear independent evidences which would enhance their significance. During the inversion with the various initial models we noted a tendency of inverted models to be smoother than the original ones. We therefore, tested whether the inversion could be still improved by using a smooth start model. For this purpose we generated a new start model applying a third order polynomial interpolation of the velocities extracted from the median model which had been obtained with start model 4, and using a Moho depth of 30 km. Using a discretized version of this smooth model, with layers each 1 km thick, as initial guess, we obtain the velocity model shown in Fig. 10(b). As before, the overall shape of the initial model is maintained, that is, the inverted model is smooth, too. However, the goodness of fit is the best of all the models treated here. In other words, from the viewpoint of the traveltime fits of the earthquakes considered here, the existence of the discontinuities at 4, 10 and even at 20 km appears questionable.

Strong discontinuities in a velocity model tend to 'attract' hypocentre locations which is an undesired effect introducing biases to the earthquake location. We suspect that also our results obtained with the optimum model 4 is affected by artificial accumulations of foci, in particular at depth around 10 km. This artefact widely

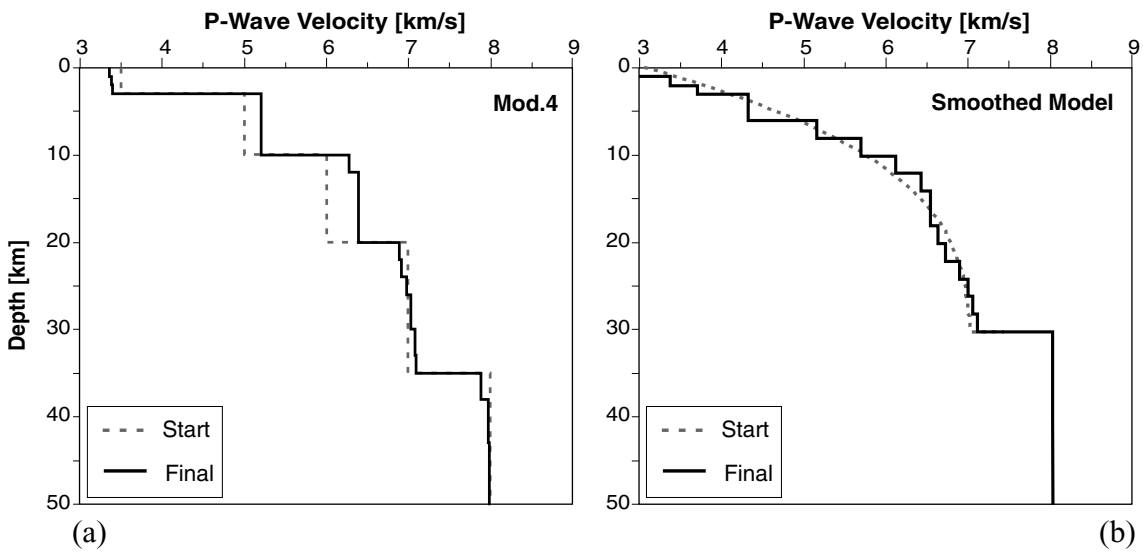

Figure 10. Comparison between start and final models: a) model 4; b) smoothed model.

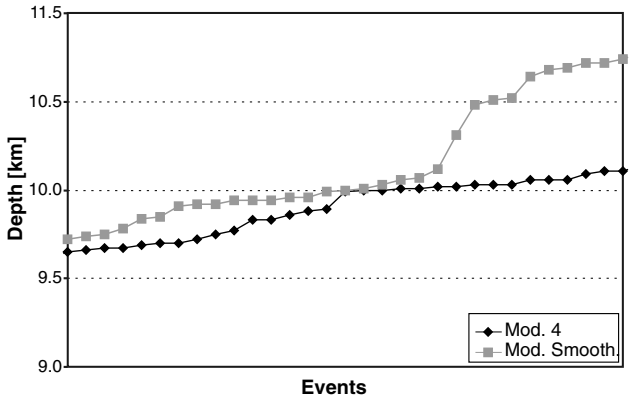

Figure 11. Ranked hypocentre distribution as a function of depth. In model 4 we find 31 hypocentres inside a strip with a width of less than 500 m in a depth around 10 km. In the smoothed model the depth dispersion of these events is about three times larger.

disappears when using the optimum smoothed model (Fig. 11). The use of smoothed models is certainly preferred in relative location techniques as these may be sensitive to the choice of unsuitable velocity models and the presence of discontinuities (see Michelini & Lomax 2004). We applied the double difference location method ('HypoDD') by Waldhauser & Ellsworth (2000) to the same data set as used for our inversion. Choosing a damping parameter of 20 we achieved a reasonable numerical stability of the method. We find that basic characteristics of the locations are maintained, even though the hypocentres appear more clustered when located with the double difference method (Fig. 12). Note the depth interval between about 18 and 30 km, where hypocentres are essentially absent. This depth range coincides pretty well with the zone where shear strength can be supposed to be controlled by the ductile behaviour of rock (see Fig. 9).

The advantages of a smooth velocity model in relative location is evident when details of the geometry of an earthquake cluster are investigated. In order to demonstrate this we have reconsidered the 'CS' cluster of hypocentres close to the village of Castroreale, which were also analysed in Scarfi *et al.* 2005. This cluster is situated in a depth where rapid changes of velocities along a gradient or velocity jumps at a discontinuity are both reasonable assumptions. We relocated the events of the cluster applying the double difference method and compared the results with two velocity models: (i) the final solution obtained with the start model 4 and (ii) the one obtained with the smooth start model and a Moho depth at 30 km. As we have been using traveltimes pickings obtained from cross-spectral analysis (for details see Scarfi *et al.* 2005), we run the code in the LSQR-mode with the lowest possible damping value of 1. In the first case we note a cluster with a somewhat unclear geometry: most of the hypocentres seem to follow a northeast striking element, whereas two foci, however, cannot be inserted in this geometry though not being identifiable as clear outliers (Fig. 13a). With the smooth model the goodness of fit of the HypoDD location improves significantly, as rms-residuals decrease from 0.014 to 0.010 s. We again find a northeast striking element, now with all foci fitting to this geometry (Fig. 13b). Note that a similar geometry of this cluster was obtained by Scarfi *et al.* (2005) by applying the master event technique of Fremont & Malone (1987) to this earthquake family. In Table 4 we summarize the cluster geometry by calculating the covariance matrix of the hypocentres obtained with the two velocity models. With the smooth model the scatter is smaller, besides this we note a clear prevailing direction inferred from the largest eigenvalue and its eigenvector.

DISCUSSION AND CONCLUSION

In absolute as well as relative earthquake location the velocity parameters are assumed to be known, that is, they are kept fixed to *a*

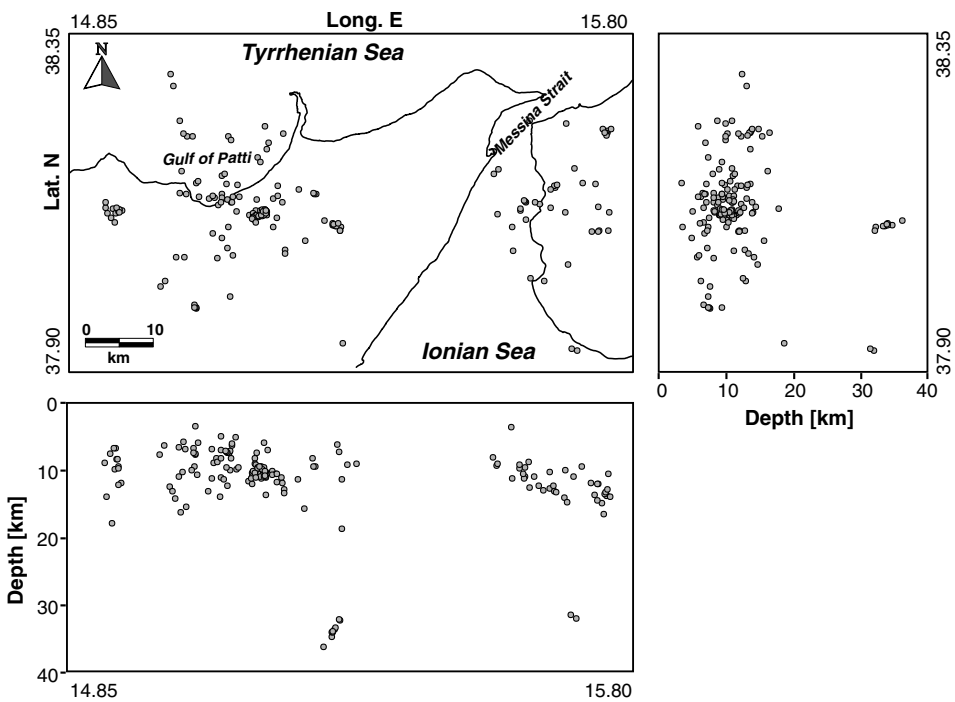

Figure 12. Map view, N–S and E–W cross-sections of the 181 hypocentres belonging to our data set (grey circles). Location was carried out with HypoDD code using the final smoothed model.

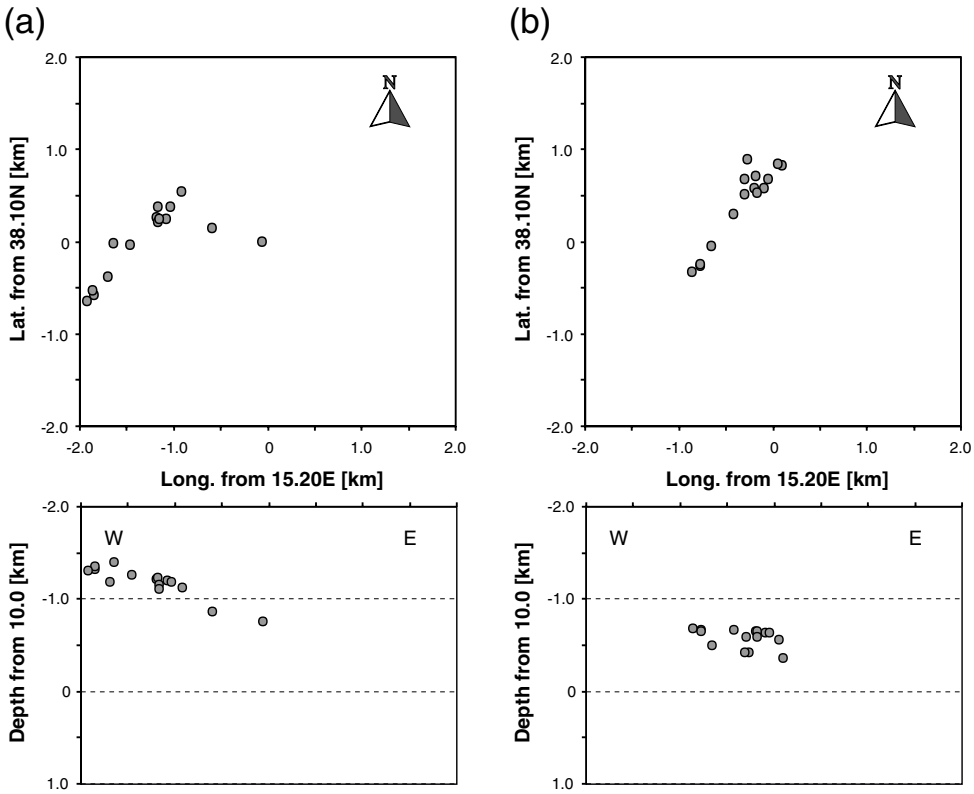

Figure 13. Map view and E–W cross-section of the 'CS' cluster. Relative location was carried out with HypoDD code using: (a) the optimum model 4 and (b) the final smoothed model (see text for further explanation).

Table 4. Eigenvalues (λ) and eigenvectors (e^T) of of the covariance matrix of relative locations (CS-cluster).

Smooth model with crude discretization				Smooth model with fine discretization			
λ (km^2)	e^T			λ (km^2)	e^T		
0.3613	0.5113	0.8268	0.2344	0.2732	0.6405	0.7629	0.0878
0.0704	0.8434	−0.4305	−0.3215	0.0106	−0.4879	0.3159	0.8137
0.0024	0.1649	−0.3621	0.9174	0.0057	0.5931	−0.5640	0.5746

Notes: The three components of the eigenvectors are the direction cosines measured to the three axis x_1 (E–W), x_2 (N–S), x_3 (vertical). The crude discretization corresponds to a thickness of the layers around the cluster of 1 km, in the fine discretization the corresponding thicknesses are 0.3 km.

priori values. The use of an inappropriate velocity model, however, can introduce systematic errors into hypocentre location (Thurber 1992; Eberhart-Phillips & Michael 1993), which strongly depend on the assumed *a priori* velocity structure (Kissling *et al.* 1995; Michelini & Lomax 2004). In the study presented here, we carry out a simultaneous inversion of hypocentre coordinates and a 1-D velocity structure using earthquakes recorded in the Peloritani Mountains in NE-Sicily and SW-Calabria. We limited ourselves to the inversion of a 1-D model, as the density of the seismic network operating in the area is still scarce. We followed the scheme introduced by Kissling *et al*. (1995), and focus our attention to the problem of the choice of an initial guess for both the velocity parameters as well as the hypocentre coordinates.

In a first series of tests, we analysed the problem of finding good start solution for the hypocentre locations. In particular, we investigated whether certain events had unstable locations bringing the risk of introducing biases to the inverted velocity model. The stability of the hypocentre locations were tested by shifting randomly five times their initial values and comparing the original locations and the final relocations achieved starting from the perturbed initial hypocentres. We excluded events for which the location differences were, in the worst case, above 3 km in the horizontal and vertical directions.

We considered eight initial *a priori* models, which had been set up and used in previous studies (De Luca *et al.* 1997; Scarfi *et al.* 2005). On the base of the overall traveltime residuals, we identified three models, for which the inversion gives similar values for the goodness of fit (i.e. models 4, 5 and 8).

The accuracy and stability of any kind of inverted model parameters is limited by the fact that the available data set is always finite. We assessed this effect by carrying out a bootstrap resampling of the earthquake catalogue, using the *a priori* model 4 as initial guess. We considered 80 realizations of resampled catalogues and estimated the variability of the obtained model parameters. Velocities are noted to change in the order of about ± 100 m s^{-1} in the upper 20 km and ± 200 m s^{-1} in the deeper parts of the model. We also note a remarkable change of the shape of the statistical distribution, which is found to be more or less Gaussian in the parts with depth <20 km,

whereas the skewness and curtosis tend to augment at greater depth. As a possible explanation we may quote the fact that most of the events are concentrated at depth less than 20 km. As a consequence the ray densities for greater depth decreases and sampling quality of the deeper parts of the model is less.

We further assess the stability of our inversion exploiting the resampled catalogues in a cross-validation test, where we compare location results of sampled and non-sampled events. This helps us to understand whether our model, whose structure is fixed *a priori*, suffers from overfitting, that is, gives reasonable errors only for the data used during the inversion, but gives unstable results if applied to extra-sample data, even if these belong to the same parent population. This may happen particularly when the number of degrees of freedom of the model is chosen too large. In our case, the comparison of bootstrap runs, where events were sampled and those where they were not sampled events, gives almost coinciding results, both with considering global parameters and looking at the single events themselves (Fig. 8). We may conclude that the number of degrees of freedom is conservative in the sense that problems of overfitting can be excluded and the application of the inverted model to new data should give stable results.

During the various inversions carried out here we noted a general tendency that the final results maintain basic characteristics of the initial models, such as major velocity jumps assumed *a priori* (i.e. the discontinuities at 4, 10 and 20 km as well as the Moho depth in our model 4). In a re-evaluation of our results we focus on two aspects: (i) an improved guess for the depth of the Moho, for which our inversion did not offer a reasonable stability and (ii) the internal structure of the more superficial layers, in particular the significance of the shallower velocity jumps (such as the ones mentioned in the model 4).

From the depth distribution of earthquake foci and considerations of the rheological characteristics of rock we may gain a reasonable guess for the Moho depth. In fact, the presence of foci between 30 and 40 km is indicative for a layer where the shear strength of the material is controlled by its brittle behaviour. We explain this by the chemical composition of rock, which is supposed to change from sialic to mafic underneath the Moho.

The velocity parameters in the bootstrap experiment using the initial model 4, cluster around median values, which are close to the ones obtained as final solution of the inversion without bootstrapping. All models obtained during the bootstrap test tend to maintain basic characteristics of the start model, in particular the position of the discontinuities at depths of 4, 10 and 20 km, for which we do not have clear *a priori* evidences. On the other hand, from the 25 and 75 per cent quantiles of the velocity models, we note a tendency towards a smoothing of these discontinuities. In other words, we question their significance as they may simply reflect the influence of the *a priori* model. In order to check whether a still better solution can be found, we have generated a new smooth starting model, carrying out a third order polynomial interpolation of velocities extracted from the median model, and fixing the Moho depth at 30 km. Using a discretized version of this smoothed starting model, we obtain the velocity structure plotted in Fig. 10b. As before, the overall shape of the initial model is maintained, that is, the inverted model is smooth, too. However, the goodness of fit (0.095 s) is the best of all models treated here. In other words, from the viewpoint of traveltime fits of the earthquakes considered here, the existence of the discontinuities at 4, 10 and even 20 km appears questionable.

Strong discontinuities in a velocity model tend to 'attract' hypocentre locations which is an undesired effect introducing biases to the earthquake location. We suspect that also our results obtained with the optimum model 4 is affected by artificial accumulations of foci, in particular at depth around 10 km. This artefact widely disappears when using the optimum smoothed model (Fig. 11). The use of smoothed models is certainly preferred in double difference relative location techniques as these may be sensitive to the choice of unsuitable velocity models and the presence of discontinuities (see Michelini & Lomax 2004). These effects can be extremely disturbing when the geometry of earthquake clusters is analysed in detail. Reconsidering an earthquake multiplet analysed in Scarfi *et al*. (2005) we demonstrate how the presence of velocity jumps may affect the geometrical properties of hypocentre clusters (Fig. 13). With a smooth model these effects disappear and the double difference location returns a pattern congruent with the one obtained by Scarfi *et al*. (2005), and which is in agreement with fault plane solutions calculated for the larger events of the cluster.

After all, we believe that the smoothed velocity model is the more suitable one for our purposes. Actually the only well-confirmed discontinuity (in depth range of concern here) is the Moho, whereas the more shallow ones are often argued. On the other hand, even if these discontinuities are physically real one may doubt about the accuracy of our information about their position in the area studied here. Thus, the smoothed model also reflects to some degree the uncertainty concerning this issue.

The differences of the velocity structure obtained with different starting models is larger than those encountered during the bootstrap test. This underscores the importance of the choice of the initial guess. This is not an easy task: often the *a priori* information concerning the position of discontinuities as well as the depth-dependency of velocities of various rock types are rather vague. From Table 1, we learn that neither the performance of a start model during standard location provides a reliable guide-line. For instance, start model 8 gave the second worst initial rms but turned out as one of the best choices with respect to the final goodness of fit. Fortunately the effects of the uncertainties discussed here on the final locations turned out as not dramatic. The scatter of the locations for the various starting models was less than 1 km for the horizontal coordinates and less than 2 km for the depth.

ACKNOWLEDGMENTS

We wish to thank two anonymous rewievers for their constructive criticism. Helpful suggestions by the associate editor, Torsten Dahm are greatly appreciated, too.

REFERENCES

Barberi, G., Cosentino, M.T., Gervasi, A., Guerra, I., Neri, G. & Orecchio, B., 2004. Crustal seismic tomography in the Calabrian Arc, *Phys. Earth Planet. Int.,* **147,** 297–314.

Billi, A., Barberi, G., Faccenna, C., Neri, G., Pepe, F. & Sulli, A., 2006. Tectonics and Seismicity of the Tindari Fault System, southern Italy: Crustal Deformations at the transition between ongoing contractional and extensional domains located above the edge of a subducting slab, *Tectonics,* **25,** TC2006, doi:10.1029/2004TC001763.

Caltabiano, T., Condarelli, D., Gresta, S., Patanè, D. & Patanè, G., 1986. Analisi preliminare dei dati della stazione sismica di Serra Pizzuta Calvarina, *CNR-IIV Open File Report,* 10/86.

Cernobori, L., Hirn, A., McBride, J.H., Nicolich, R., Petronio, L. & Romanelli, M., 1996. Crustal image of the Ionian basin and its Calabrian margins, *Tectonophysics,* **264,** 175–189.

D'Agostino, N. & Selvaggi, G., 2004. Crustal motion along the Eurasia-Nubia plate boundary in the Calabrian Arc and Sicily and active extension in the Messina Straits from GPS measurements, *J. Geophys. Res.,* **109,** B11402, doi:10.1029/2004JB002998.

De Luca, G., Filippi, L., Caccamo, D., Neri, G. & Scarpa, R., 1997. Crustal structure and seismicity of southern Tyrrenian basin, *Phys. Earth Planet. Int.,* **103,** 117–133.

Dezes, P. & Ziegler, P.A., 2001. European Map of the Mohorovicic discontinuity. *2*nd *EUCOR-URGENT Workshop* (Upper Rhine Graben Evolution and Neotectonics). Mt. St., Odile, France.

Dziewonski, A.M., Ekström, G., Franzen, J.E. & Woodhouse, J.H., 1987. Global seismicity of 1978: centroid-moment tensor solutions for 512 earthquakes, *Phys. Earth Planet. Int.,* **46,** 316–342.

Eberhart-Phillips, D. & Michael, A.J., 1993. Three-dimensional velocity structure, seismicity, and fault structure in the Parkfield region, central California, *J. Geophys. Res.,* **98,** 737–758.

Efron, B., 1982. *The Jackknife, the Bootstrap, and Other Resampling Plans*, Society of Industrial and Applied Mathematics, Philadelphia, CBMS-NSF Monographs, pp. 38.

Finetti, I. & Del Ben, A., 1986. Geophysical study of the Tyrrhenian opening, *Boll. Geof. Teor. Appl.,* **110,** 75–155.

Frémont, M.J. & Malone, S.D., 1987. High precision relative locations of earthquakes at Mt. St. Helens, Washington, *J. Geophys. Res.,* **92,** 10 223–10 236.

Gasparini, C., Iannaccone, G. & Scarpa, R., 1985. Fault plane solutions and seismicity of the Italian peninsula, *Tectonophysics,* **117,** 59–78.

Goetze, C., 1978. The mechanisms of creep in olivine, *Phil. Trans. Roy. Soc. London*, **288,** 99–119.

Hastie, T., Tibshirani, R. & Friedman, J., 2002. *The Elements of Statistical Learning*, Springer-Verlag, Berlin, pp. 533.

Hesterberg, T., Monaghan, S., Moore, D.S., Clipson, A. & Epstein, R., 2003. Bootstrap and permutation tests – Companion chapter 18 to the "Practice of Business Statistics", in *The Practice of Business Statistics*, Freeman, W. H. & Co., New York.

Husen, S., Kissling, E., Flueh, E. & Asch, G., 1999. Accurate hypocenter determination in the seismogenic zone of the subducting Nazca plate in north Chile using a combined on-/offshore network, *Geophys. J. Int.,* **138,** 687–701.

Kissling, E., Ellsworth, W.L., Eberhart-Phillips, D. & Kradolfer, U., 1994. Initial reference models in local earthquake tomography, *J. Geophys. Res.,* **99,** 19 635–19 646.

Kissling, E., 1995. *Velest User's Guide*, Internal Report, Institute of Geophysics, ETH, Zurich, pp. 26.

Kissling, E., Solarino, S. & Cattaneo, M., 1995. Improved seimic velocity reference model from local earthquake data in Northwestern Italy, *TerraNuova*, **7,** 528–534.

Laigle, M., 1998. Images sismiques de l'Etna à diverses èchelles: Nouveaux éléments sur son comportement et le cadre règional, *PhD thesis*, University of Paris 7, Paris, pp. 288.

Lentini, F., Catalano, S. & Carbone, S., 2000. *Carta geologica della provincia di Messina*, Provincia Regionale di Messina. Assessorato Territorio–Servizio geologico, SELCA, Firenze.

Michelini, A. & Lomax, A., 2004. The effect of velocity structure errors on double-difference earthquake location, *Geophys. Res. Lett.,* **31,** L099602, doi:10.1029/2004GL019682.

Monaco, C. & Tortorici, L., 2000. Active faulting in the Calabrian Arc and eastern Sicily, *J. Geodyn.,* **29,** 407–424.

Neri, G., Barberi, G., Orecchio, B. & Aloisi, M., 2002. Seismotomography of the crust in the transition zone between the southern Tyrrhenian and Sicilian tectonic domains, *Geophys. Res. Lett.,* **29**(23), 2135, doi:10.1029/2002GL015562.

Neri, G., Barberi, G., Orecchio, B. & Mostaccio, A., 2003. Seismic strain and seismogenic stress regimes in the crust of the southern Tyrrhenian region, *Earth Planet. Sci. Lett.,* **213,** 97–112.

Neri, G., Barberi, G., Oliva, G. & Orecchio B., 2005. Spatial variations of seismogenic stress orientations in Siciliy, South Italy, *Phys. Earth Planet. Int.,* **148,** 175–191.

Nicolich, R., Laigle, M., Hirn, A., Cernobori, L. & Gallart, J., 2000. Crustal structure of the Ionian margin of Sicily: Etna volcano in the frame of regional evolution, *Tectonophysics,* **329,** 121–139.

Scarfi, L., Langer, H. & Scaltrito, A., 2005. Relocation of microearthquake swarms in the Peloritani mountains – implications on the interpretation of seismotectonic patterns in NE Sicily, Italy, *Geophys. J. Int.,* **163,** 225–237, doi: 10.1111/j.1365-246X.2005.02720.x.

Sgroi, T., Braun, T., Dahm T. & Frugoni F., 2006. An improved seismicity picture of the Southern Tyrrhenian area by the use of OBS and land-based networks: the TYDE experiment, *Ann. Geophys.,* **49**(2/3), 801–817.

Stüwe, K., 2002. *Geodynamics of the Lithosphere*, Springer-Verlag Berlin Heidelberg, pp. 449.

Thurber, C.H., 1992. Hypocentre–velocity structure coupling in local earthquake tomography, *Phys. Earth Planet. Int.,* **75,** 55–62.

Waldhauser, F. & Ellsworth, W.L., 2000. A double-difference earthquake location algorithm: Method and application to North Hayward Fault, California, *Bull. Seism. Soc. Am.,* **90,** 1353–1368.

Wells, D.L. & Coppersmith, J., 1994. New empirical relationships among magnitude, rupture length, rupture width, rupture area and surface displacement, *Bull. Seism. Soc. Am.,* **84,** 974–1002.